

APPLICATION OF ILLUMINATED LOCK-IN THERMOGRAPHY TO INDUSTRIAL SILICON SOLAR CELLS

W. Kwapil, M. Kasemann, J. Ebser, S. Rein & W. Warta
 Fraunhofer ISE, Freiburg, Germany
 Heidenhofstr. 2, 79110 Freiburg, Germany

ABSTRACT: Illuminated lock-in thermography (ILIT) was introduced for spatially resolved measurement of the local power dissipation in a solar cell. For this paper, industrial silicon solar cells were processed and ILIT images taken after each process step, starting with the emitter diffusion. Non ideal processing during the wafer texturization, the contact firing and the laser edge isolation was intentionally applied in order to show the influence of the various dissipation channels in ILIT images. As a result, it is shown that edge shunts due to low laser edge isolation quality are only visible in ILIT MPP images if the global R_p is lower than approximately $1 \text{ k}\Omega\text{cm}^2$.

Keywords: ILIT, characterization, shunts

1 INTRODUCTION

Illuminated lock-in thermography (ILIT) was introduced as a powerful and versatile tool [1,2] that is able to detect regions with insufficient metal-emitter contact as well as ohmic and non-linear shunts in solar cells. Since both, the quality of the metal-emitter contact and the location and strength of shunts are important pieces of information for the evaluation of industrial solar cell processing, ILIT seems to be a valuable tool for the quality control of an industrial process line.

The underlying physical principle of illuminated lock-in thermography has been described in detail elsewhere [1-4]. Thermography measures the heat generated via various power dissipation channels, modified by the local emissivity of the wafer surface. Most of the power dissipation channels are affected by the local emitter voltage or the resulting electric fields.

So far, most of the published work has covered ILIT measurements of single solar cells with well defined issues, see e.g. [5,6]. In this contribution, we investigate a large quantity of standard industrial silicon solar cells, some of them non ideally processed. By comparing the ILIT images of the cells with each other, we try to differentiate between competing power dissipation mechanisms. Therefore, a batch of wafers was processed at the Photovoltaic Technology Evaluation Center (PV-TEC) at Fraunhofer ISE, where processing conditions are comparable to the photovoltaic industry.

For this batch, multicrystalline wafers and Cz wafers were taken and laser marked, followed by a standard industrial solar cell process. A sketch of the process is shown in Fig. 1. Non ideal processing was applied to an assortment of wafers on several levels: The alkaline texture, the contact firing, and the laser edge isolation (highlighted in orange). Additionally, some cells were intentionally shunted after the processing.

ILIT measurements were taken after POCl diffusion, after POCl etch, after contact firing and after laser edge isolation. If not indicated otherwise, all of the following ILIT images present the -90° measurements with the same scales as shown in Fig. 2, only depending on whether the wafers are textured or not (independent of material or process step).

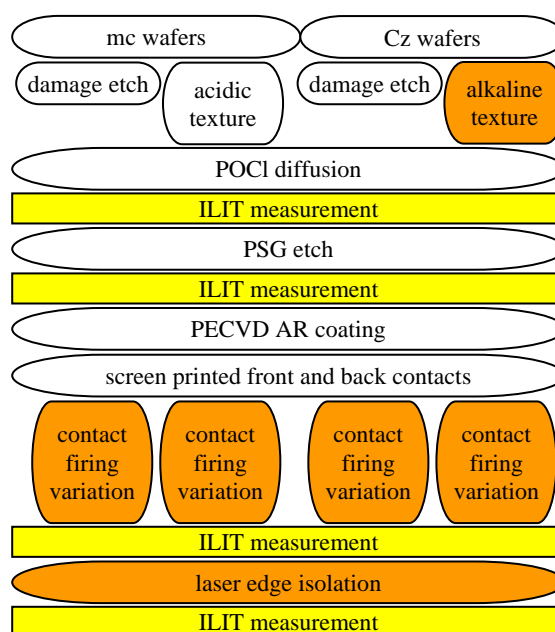


Figure 1: Flow chart of the standard industrial solar cell process used in this work. During the process steps that are highlighted in orange, non ideal conditions were applied to part of the wafers.

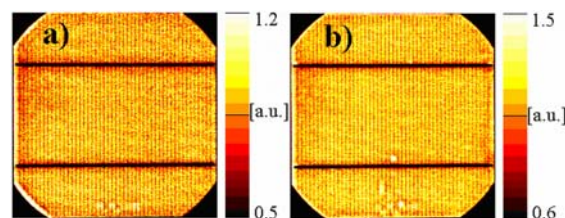


Figure 2: V_{oc} ILIT images of two Cz solar cells which were a) damage etched or b) textured. Note the two different scales which have been used throughout this work. The features at the bottom are shunts due to the laser marking of the wafers.

2 INFLUENCE OF VARYING EMISSIVITY

ILIT measurements are largely influenced by the emissivity of the wafer surface. In some cases, emissivity variations dominate the ILIT signal and make interpretation of the measurements difficult. The surface emissivity depends on several factors: the wafer material,

the grain orientation, the dopant concentration in base and emitter, and the surface morphology. In general, the emissivity of textured wafers is higher than that of damage etched wafers (see Fig. 2).

Figure 3 shows ILIT measurements in J_{sc} -, MPP- and V_{oc} -mode of the same monocrystalline cell. Residues on the wafer surface before the alkaline texturization process led to an inhomogeneous surface morphology which in turn is responsible for the dark oval features in all three ILIT measurements.

Since the emissivity depends only to a small extent on the voltage of the cell, one can estimate the influence of an inhomogeneous emissivity on ILIT measurements by comparing images in different measurement modes with each other.

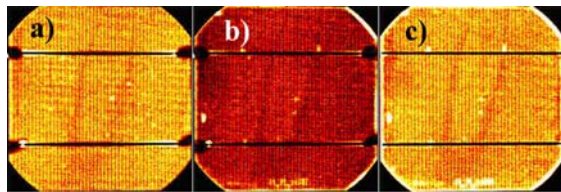


Figure 3: Influence of emissivity on ILIT measurements in a) J_{sc} , b) MPP and c) V_{oc} mode of the same cell. The dark oval shape is due to inhomogeneous wafer texturization and can be seen in all measurement modes.

3 MEASUREMENTS AFTER DIFFUSION AND AFTER PSG ETCH

One advantage of ILIT measurements is that they can already be performed on diffused wafers. Thus, quality control by ILIT can begin right after the emitter diffusion step.

POCl glass which resides on the wafer surface after emitter diffusion leads to an increased emissivity compared to wafers after the PSG etch. Apart from that, we have seen no other influence on the ILIT measurements. Therefore, in order to keep surface contamination at a minimum, it is advantageous to take the ILIT images directly after diffusion since the wafers are not as sensitive at this stage as after the PSG etch.

4 QUALITY OF METAL-EMITTER CONTACT

Figure 4 shows a compilation of ILIT measurements in J_{sc} (column A), MPP (column B) and V_{oc} (column C) mode of mc solar cells whose metal-emitter contacts are of varying quality due to the different peak contact firing temperatures applied. Cells with underfired front contacts (row 1) display a large similarity between all three ILIT images. Even the measurement made under J_{sc} -conditions (1A) exhibits features that are to a large extent similar to the V_{oc} measurement (1C). In contrast, the J_{sc} image of cells with well fired front contacts (row 3) shows almost a laterally uniform signal. In the V_{oc} measurement (3C), the contrast between regions of high recombination and their surroundings is increased while the MPP image (2C) displays a very low signal over the whole wafer area. Cells with partly fired front contacts (row 2) exhibit features of both, underfired and well fired contacts. The badly contacted regions in the MPP image (2B) at the right resembles the corresponding areas of the sister cell that was underfired (1B). In the J_{sc} image (2A), the bright spots are due to ohmic losses in the series resistance and

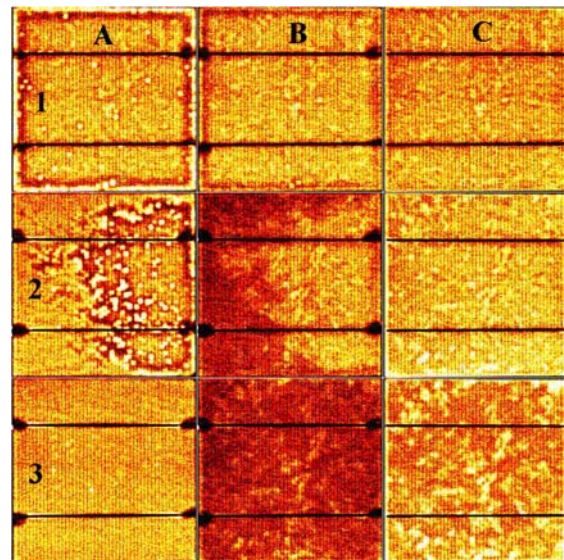


Figure 4: ILIT measurements in J_{sc} (column A), MPP (column B) and V_{oc} (column C) mode. Three different peak temperatures during contact firing were applied (cell 1 = lowest, cell 3 = highest temperature).

indicate randomly contacted spots in a badly contacted area. Here, the influence of material defects cannot be seen.

As has been explained in [1], the different power dissipation channels depend on the local emitter potential which in turn depends on the quality of the metal-emitter contact. If the front grid is electrically well contacted to the emitter, i.e. if the contact resistance is low, also the potential drop between grid and emitter is low. Then the external electric load determines the emitter potential. This is the reason for the large differences between the J_{sc} (column A) and MPP (column B) images of the different cells. In fact, although the *grid potential* of the cell with underfired front contacts (row 1) is pinned to 0 V or to approx. 0.5 V (J_{sc} and MPP, respectively) by the external load, the *emitter potential* of a large part of the wafer is as large as under open circuit conditions, resulting in very similar J_{sc} , MPP and V_{oc} images. Only at the edges, there is an electric contact between grid and emitter. This leads to ohmic losses at the edges in J_{sc} mode (bright signal in image 1A).

In the badly contacted area of the MPP image 2B (right half), the same material-induced features as in image 1B can be seen at almost the same background signal level. The drop in the emitter potential between badly contacted and well contacted regions is not as instantaneous as image 2B might suggest. Linescans of MPP measurements of partly contacted cells show that the ILIT signal increases slowly coming from the well contacted area of the cell (see Fig. 5). If the potential drop were more drastic, one would expect a larger gradient in the ILIT signal of well contacted and badly contacted areas.

A second aspect which comes with good metal contacting is that it leads to enhanced lateral distribution of the electrons that have crossed the *pn* junction because in this case they can travel through the grid. Thus, if the cell is connected to an external electric load, most of the electrons are drained from the regions whose metal-emitter contact is good. In MPP measurements, the electric load drains the maximum power; therefore the

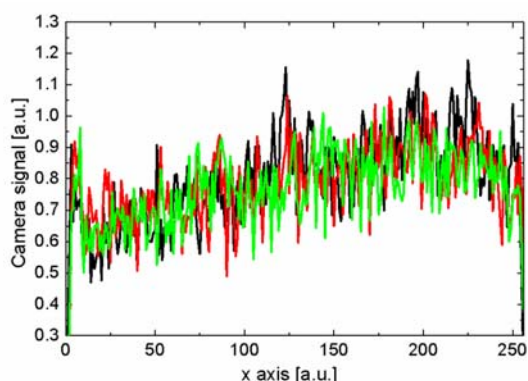


Figure 5: Linescans through the middle of the MPP ILIT images of three mc solar cells (damage etched) whose metal grid is only partly contacted to the emitter (compare to Fig. 4, row 2). The signal increases almost linearly from the well contacted (left) to the non contacted (right) part of the cell.

ILIT signal is lowest in this mode. On the other hand, even if the cell is in open circuit, the electrons in the grid can travel over large distances and follow the electric field. Local potential drops caused by recombination currents (or shunts) can therefore attract majority carriers of a large part of the cell. This effect can be seen clearly in the V_{oc} image 3C of the well contacted cell. Here, the areas with a bright ILIT signal due to material defects are more pronounced than in the V_{oc} images 1 and 2C.

5 LASER EDGE ISOLATION AND OTHER SHUNTS

Before the laser edge isolation step (LEI), the emitter and the screen printed aluminium backside are in direct contact, leading to large shunt currents which can be seen in the ILIT images. The influence of these shunts on the current distribution depends on the quality of the metal-emitter contact, too, as we have explained in the last paragraph.

Figure 6 shows ILIT measurements of the same cells as Fig. 4, but before the laser edge isolation was done. The edge shunts cause bright signals in the MPP and V_{oc} -mode whereas the J_{sc} -images (left row) resemble those after laser edge isolation, see Fig. 4.

Interesting are the darker regions beside the edge shunts in all parts where the metal-emitter contacts were not formed. In fact, these regions of lower ILIT signal seem to always adjoin the location of shunts or recombination currents if the electrons cannot travel through the grid, e.g. around material defects in mc wafers after POCl diffusion. In these cases, the electrons can only travel through the emitter.

Then, if there is a strong shunt which causes the local emitter potential to drop, the potential gradient around the shunt is determined by the emitter sheet resistance surrounding the shunt. Those electrons that feel the potential gradient are drawn towards the shunt and most of them recombine there. The ILIT signal around a shunt can then be attributed to at least three competing effects:

- Majority carriers are drained to the shunt,
- a lower emitter potential increases the pn -junction thermalization heat,
- the currents towards the shunt cause Joule heating.

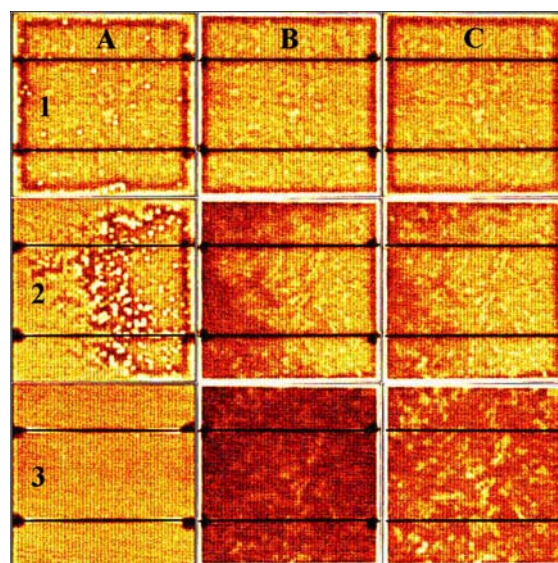


Figure 6: ILIT measurements of the same cells as in Fig. 4 before the laser edges were isolated. Column A: J_{sc} , column B: MPP, column C: V_{oc} .

Since the second and third effects should both increase the ILIT signal close to a shunt, the major effect leading to a low ILIT signal is the lower bulk recombination heat due to a local lack of carriers.

In a solar cell with good metal-emitter contacts (cell 3), majority carriers from the whole area of the cell can be drawn towards a shunt, depending on the strength of the shunt and its spatial extension, the series resistance between the emitter and the grid and the series resistance within the metal fingers. The large edge shunt lowers therefore the V_{oc} signal level over the entire cell. This fact can be seen by comparing image 3C of Figures 4 and 6. Additionally, the edge shunt of cell 3 shows a larger ILIT signal than the shunt of cell 1 (images 3C and 1C, respectively), since in the former case, the electrons move through the grid, in the latter through the emitter. The strength of the shunt signals therefore do not depend only on the IV characteristics of the shunt (ohmic or diode-like) and its strength but also largely on the current density that reaches the shunt.

In order to illustrate the influence of the series resistances of the emitter-metal contact and within the grid on shunt recombination currents, a cell was strongly shunted at the end of one busbar, see Fig. 7. The shunt resistance of this cell is below $100 \Omega\text{cm}^2$ after shunting. In fact, this shunt is so strong that it can even be seen in one single IR camera image, not necessitating the lock in

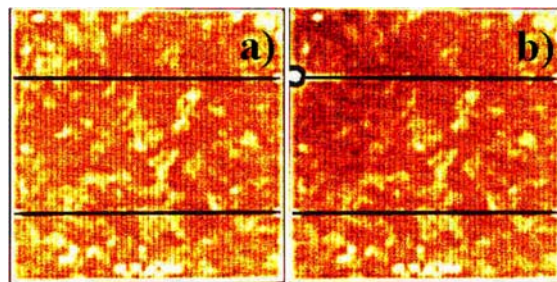


Figure 7: ILIT measurements in V_{oc} mode of mc solar cell 4 (textured) which was contact fired at 900°C a) before and b) after shunting. This strong shunt was created at one end of a busbar by a dielectric breakdown.

principle. The shunt current is visibly drawn from more than one quarter of the whole cell area, at the same time suppressing bulk recombination heat in this part. Far away from the shunt, the ILIT signal seems to be unaffected. The large current density flowing to the shunt through the busbar increases the ILIT signal at the busbar close to the position of the shunt due to Joule heating [3].

6 ASSESSMENT OF LASER EDGE ISOLATION QUALITY

Before and after the laser edge isolation, the IV-characteristics of all cells were measured. In this section, the resulting data shall be used to give an idea about the correlation between the ILIT images and the solar cell parameters. The question is whether it is possible to assess the quality of any industrial solar cell by looking at ILIT measurements only.

Shunt resistances are best seen if influences of the series resistance and of leakage currents (J_{02}) due to material defects are suppressed. These conditions are best fulfilled simultaneously around the maximum power point [6]. Of course, measurements at the MPP have the additional advantage of imitating the real working conditions of the solar cell.

Before laser edge isolation, all cells have a shunt resistance below $100 \Omega\text{cm}^2$ and the shunted edges are clearly seen in the MPP image, Fig. 8 a). By varying the laser power, the laser edge isolation of these three cells results in different shunt resistances and thus, different fill factors. Although shunt resistances below $3 \text{ k}\Omega\text{cm}^2$ have an influence on the fill factor [8], ILIT images of

Table I: Shunt resistance (R_p) and fill factor (FF) of cells which have seen non ideal laser edge isolation, see Fig. 8

Cell no.	R_p (Ωcm^2)	FF (%)
5	240	71.9
6	940	77.2
7	2500	77.9

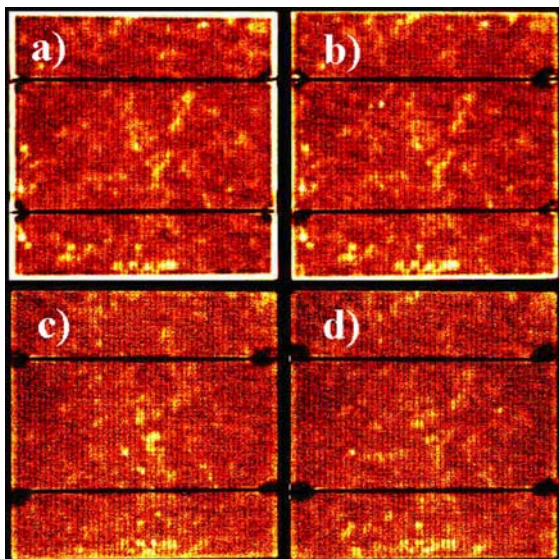


Figure 8: MPP-ILIT images of three mc solar cells (textured) fired at 900°C . a) Cell 5 before laser edge isolation, measured $R_p=90 \Omega\text{cm}^2$, b) cell 5 after laser edge isolation, $R_p=240 \Omega\text{cm}^2$, c) cell 6 after LEI, $R_p=940 \Omega\text{cm}^2$, d) cell 7 after LEI, $R_p=2500 \Omega\text{cm}^2$.

cells with shunt resistances above approximately $1 \text{ k}\Omega\text{cm}^2$ show hardly any signal at the edges, see Fig. 8 c) and d). Only cell 5 with a shunt resistance of $240 \Omega\text{cm}^2$ shows a distinctly bright lower edge. Note that the power which is dissipated by shunting with $R_p > 1 \text{ k}\Omega\text{cm}^2$ is minimal which can be seen in the corresponding values of the FF.

Another reason for these findings might also be that part of the heat radiation generated at the edge of the cell can be irradiated into a larger solid angle due to the presence of the wafer edge. It would therefore be lost for the camera detector.

7 CONCLUSION

Illuminated lock-in thermography measurements of a large quantity of industrial solar cells were made, some of them processed intentionally under non ideal conditions. ILIT images were taken at different stages of the cell processing and in different measurement modes.

As a result, the influence of inhomogeneous surface emissivity, varying metal-emitter contacts, edge shunts of varying strength and strongly localized shunts on J_{sc} , MPP and V_{oc} measurements were shown and their physical origin were discussed. These images may help with the interpretation of ILIT measurements of any industrial silicon solar cell. It was shown that ILIT MPP images can reliably identify non ideal laser edge isolation for global R_p -values lower than approx. $1 \text{ k}\Omega\text{cm}^2$.

8 ACKNOWLEDGEMENTS

The authors acknowledge the financial support from the German Ministry for the Environment, Nature Conservation and Nuclear Safety under contract 0327616 (PVQC).

- [1] J. Isenberg, W. Warta, J. Appl. Phys **95**, 5200 (2004)
- [2] M. Kaes, S. Seren, T. Pernau, G. Hahn, Prog. Photovolt. **12**, 355 (2004)
- [3] J. Isenberg, W. Warta, Prog. Photovolt. **12**, 339 (2004)
- [4] O. Breitenstein, J.P. Rakotoniaina, J. Appl. Phys. **97**, 074905 (2005)
- [5] J. Isenberg, A.S.H. van der Heide, W. Warta, Prog. Photovolt. **13**, 697 (2005)
- [6] J. Isenberg, A.S.H. van der Heide, W. Warta, Proc. 20th EU-PVSEC, Barcelona (2005)
- [7] K. Ramspeck, P. Altermatt, N.P. Harder, R. Brendel, Proc. 21st EU-PVSEC (2006)
- [8] E. Schneiderloechner, PhD thesis, p. 132, Freiburg (2004)